



Accurate Contact-Free Material Recognition with Millimeter Wave and Machine Learning

Shuang He¹, Yuhang Qian¹, Huanle Zhang¹, Guoming Zhang¹, Minghui Xu¹,
Lei Fu^{2,3}, Xiuzhen Cheng¹, Huan Wang⁴, and Pengfei Hu¹(✉)

¹ Shandong University, Qingdao, Shandong, China
{heshuang, dtczhang, guomingzhang, mhxu, xzcheng, phu}@sdu.edu.cn

² Bank of Jiangsu, Nanjing, China
leileifu@163.sufe.edu.cn

³ Fudan University, Shanghai, China

⁴ Guangxi University of Science and Technology, Liuzhou, China
wanghuan@gxust.edu.cn

Abstract. Material recognition plays an essential role in areas including industry automation, medical applications, and smart homes. However, existing material recognition systems suffer from low accuracy, inconvenience (e.g., deliberate measuring procedures), or high cost (e.g., specialized instruments required). To tackle the above limitations, we propose a contact-free material recognition system using a millimetre wave (mmWave) radar. Our approach identifies materials such as metal, wood, and ceramic tile, according to their different electromagnetic and surface properties. Specifically, we leverage the following techniques to improve the system robustness and accuracy: (1) spatial information enhancement by exploiting multiple receiver antennas; (2) channel augmentation by applying Frequency Modulated Continuous Wave (FMCW) modulation; and (3) high classification accuracy enabled by Artificial Intelligence (AI) technology. We evaluate our system by applying it to classify five common materials. The experimental results are promising, with 98% classification accuracy, which shows the effectiveness of our mmWave-based material recognition system.

Keywords: Contact-free material recognition · Millimeter wave radar · Machine learning

1 Introduction

Recognizing materials have a wide range of applications, e.g., categorizing waste materials in industrial automation [3], detecting normal/cancerous cells in the

This work is supported by the National Key Research and Development Program of China (No. 2021YFB3100400), the Shandong Science Fund for Excellent Young Scholars (No. 2022HWYQ-038), the Guangxi Natural Science Foundation (No. 2020GXNSFBA159042).

medical field [8, 29], and modeling environments in smart homes [15]. With the development of smart city, material recognition has become an imperative component for many intelligent devices. Compared to their contact-based counterparts, contact-free material recognition systems are gaining popularity because of their fewer physical constraints and better user experience.

There are several mainstream methods to build contact-free material recognition systems. (1) Near Infrared (NIR) spectroscopy. NIR spectroscopy is a method to detect the electromagnetic spectrum from 780 nm to 2500 nm wavelengths. It has been applied to recognize many organic materials [16]. However, NIR spectroscopy has many shortcomings, such as high cost and low accuracy. (2) Optical sensing technology (e.g., lidar) uses a light resistance with multi-spectral illumination to identify the surface materials [7], but its accuracy is severely affected by the visibility degree of objects. (3) Mechanical radars rely on signal factors such as distances and incident angles to classify materials [19]. However, such sensing technology is complex and expensive, and the hardware requirements are strict. None of those mentioned above methods provides affordable and accurate contact-free material recognition functionality.

In this paper, we propose a mmWave radar system to recognize materials. Our system has the same merits of robustness and versatility as the mechanical radars have, but ours does not have the problems of complex structures and challenging operational conditions faced by mechanical radars. Compared with other frequency bands, mmWave radar achieves a supreme performance regarding accuracy, cost, and size. Specifically, an mmWave radar system has the following strength:

1. *High Resolution.* mmWave radars have high resolutions because of their excellent signal beam-forming. For example, a 76–81 GHz radar's range resolution reaches the sub-millimetre level, and the angular resolution is as precise as 1° [29, 30].
2. *Robustness.* When the visibility condition is poor, e.g., in rain and mist, the sensing performance of an mmWave radar is still robust. As a result, an mmWave system is capable of all-weather and all-time sensing.
3. *Lightweight.* Thanks to the development of microelectronic technology, mmWave radars are becoming miniature and low cost. Embedded devices and wearable devices are highly likely to incorporate mmWave radars to enable millimeter communications and sensing capability.

Although mmWave signals have incomparable advantages, realizing a practical and accurate mmWave radar system for material recognition entails careful considerations. This is because mmWave signals are susceptible to environments. Therefore, designing a robust and precise feature representation scheme for distinguishing materials is the core. To improve the material recognition accuracy, we leverage the following techniques:

1. Aggregation of multiple transmitter-to-receiver (Tx-to-Rx) paths. A typical mmWave hardware has multiple transmitter and receiver antennas. Each Tx-to-Rx pair captures different channel information. In light of it, we propose to incorporate multiple Tx-to-Rx pairs to exploit more spatial information.

2. Frequency-Modulated Continuous Wave (FMCW) modulation to measure the Received Signal Strength (RSS) of the signals reflected from a target material. Compared to a Continuous Wave (CW)-based radar, an FMCW radar enables more precise RSS profiles since it spans a frequency band.
3. A complete Machine Learning (ML) pipeline. Our system extracts useful features from the RSS profiles that are generated by multiple Tx-to-Rx pairs. Afterwards, it runs a powerful ML model to recognize the materials, which shows inspiring classification accuracy.

We evaluate our system by classifying five common building materials (copper, wood, acrylic, tile, and drywall), where an mmWave radar is placed at 40 cm from the materials. The evaluation results show the effectiveness of our system. In particular, our Convolutional Neural Network (CNN)-based pipeline achieves inspiring 98% classification accuracy.

This paper is organized in the following manner. First, we provide related works in Sect. 2. Then, we elaborate our system design in Sect. 3. Afterwards, we evaluate our system in Sect. 4. We discuss the limitations/opportunities in Sect. 5. Last, we conclude this paper in Sect. 6.

2 Related Works

This section provides related works in terms of contact-based material recognition and Radio Frequency (RF)-based contact-free material recognition.

2.1 Contact-Based Material Recognition

Several contact-based systems have been proposed to realize material recognition by utilizing physical-level features such as chemical properties [21], thermal properties [20], and optical properties [11]. Despite their industrial deployments, these solutions are task-oriented and have no mobility. Furthermore, they require to attach specified sensors to objects for recognition. In comparison, our system is a contact-free solution and thus is more flexible and user-friendly.

2.2 RF-Based Contact-Free Material Recognition

In addition to localization [1] and perception [5], signal reflection of RF waves can be used for material recognition. For example, RSA [31] determines curvature and surface material by measuring the reflected mmWave signals at multiple locations. RadarCat adopts a similar workflow but uses 60 GHz signals [28]. Yang et al. [26] investigate the feasibility of using 60 GHz millimeter-wave (mmWave) signal as a ubiquitous and non-invasive way to estimate the Soluble Sugar Content (SSC) in fruits. Beside, some other RF-based works consider more on magnetic properties (e.g., dielectric constant ϵ_r , losses $\tan\delta$ [2, 23]), which require expensive facility like vector network analyzer, with sophisticated calibrating procedures as beamforming with high-gain dielectric lenses or elliptical mirror.

In comparison, we only use one mmWave board with onboard transmitters and receivers. In addition, existing millimeter works are vulnerable to the positions of transmitters and receivers, as they rely on sensitive phase information of signals. Compared to existing mmWave works, our system exploits ML learning that extracts features from RSS profiles, which is more robust against wavelength misalignment. Besides mmWave communications, other RF technologies such as Wi-Fi [6, 13], UWB [4], and RFID [24] have been used for material classification. However, they have much lower classification accuracy in practice because of the long wavelengths and already congested frequency bands.

3 System Design

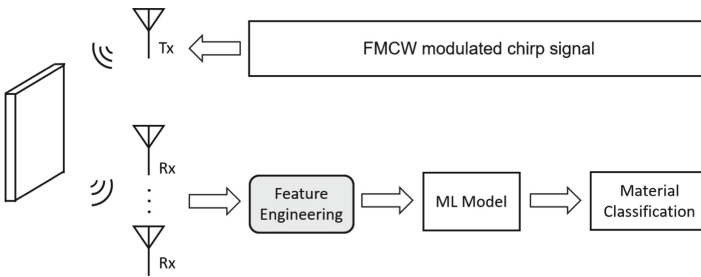


Fig. 1. The workflow of our system.

Our system recognizes materials based on the reflected mmWave signals. Figure 1 depicts the workflow of our system. An FMCW modulated chirp signal is emitted directly toward the target material for recognition, which signal is then reflected by the material and received by multiple receiver antennas. Afterward, we extract features from multiple receiver antennas (details in Sect. 3.3). Last, we adopt an ML model to classify the material.

3.1 Principle of mmWave Material Recognition

In a mono-static radar, the mmWave signal follows the propagation model [14]:

$$P_r = \frac{P_t G_t G_r \lambda^2 \sigma}{(4\pi)^3 d^4} \tag{1}$$

where P_r is the power of received signals, P_t is the transmit power, with G_t and G_r are the antenna gains for Tx and Rx respectively. λ is the wavelength transmitted in free space. Since mmWave has a short wavelength, it indicates that mmWave signals suffer severer attenuation than microwave signals. To compensate for signal attenuation, practical mmWave radars use Multiple Input Multiple Output (MIMO) antenna arrays to obtain high G_t and G_r gains.

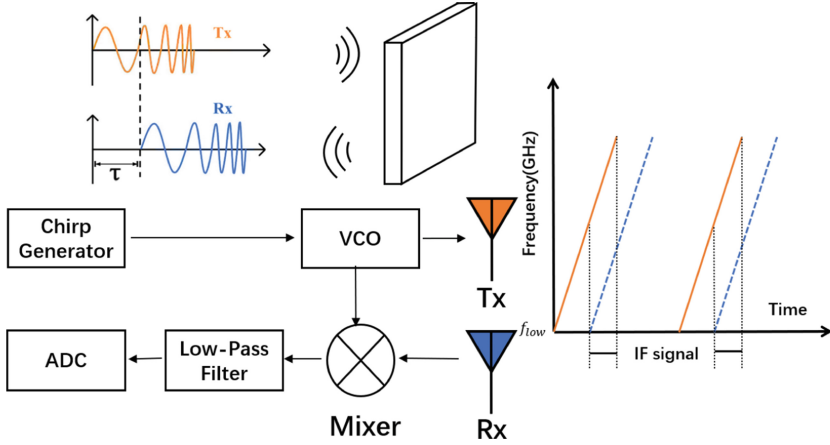


Fig. 2. Illustration of FMCW modulation.

σ is the Radar Cross Section (RCS), a metric to represent the size of an object that appears in the view of a radar. RCS can be regarded as the electromagnetic equivalent area of a target object, the area that intercepts the transmitter radar power and then scatters that power isotropically back to the radar receiver. The RCS area does not necessarily overlap with the physical area of an object. It is largely determined by the material reflectivity. For example, metal suffers a 0.6 dB RSS loss while that of wood is 12 dB. Therefore, when we measure objects in a homogeneous condition (e.g., shape, distance to the radar, radar configurations), we can leverage P_r (correspondingly σ) to classify their materials.

3.2 Channel Augmentation with FMCW Modulation

FMCW modulates signals in chirps—a sinusoidal wave signal in a linearly increasing frequency. FMCW is widely used for ranging. We adopt FMCW to augment channel information by changing the transmission frequency. Therefore, compared to a single-frequency Continuous Wave (CW) modulation, FMCW provides more detailed channel information and thus higher material recognition accuracy.

Figure 2 illustrates the FMCW modulation. For a monostatic radar, the Tx and Rx signal can be described with real numbers as

$$\begin{aligned} S_T(t) &= A_T \cdot \cos(2\pi \cdot f_T(t) \cdot t + \phi_T) \\ S_R(t) &= A_R \cdot \cos(2\pi \cdot f_R(t) \cdot t + \phi_R) \end{aligned} \quad (2)$$

where A_T and A_R are the amplitude of signal, $f_T(t)$ and $f_R(t)$ are the run-time frequency of signal at time t , ϕ_T and ϕ_R are the initial phrase of transmitted and received signal respectively. By multiplying $S_T(t)$ and $S_R(t)$, we obtain the Intermediate Frequency (IF) signal:

$$S_{IF}(t) = S_T(t) * S_R(t) \approx \frac{1}{2} A_T A_R * \cos \{ [2\pi (f_T(t) - f_R(t))] t + (\phi_T - \phi_R) \} \quad (3)$$

where a low-pass filter is applied to remove the higher frequency.

3.3 Feature Engineering

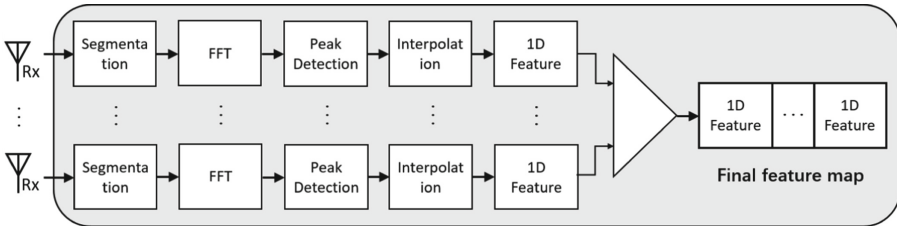


Fig. 3. The procedure of our feature engineering.

We extract features from $S_{IF}(t)$ and then apply an ML model to classify the materials based on the extracted features. Figure 3 illustrates our feature engineering procedure. Specifically, we design the following steps:

1. We segment the data stream chirp-wise, where each segment lasts 21 ms and has 64 Analogue to Digital Converter (ADC) samples. To avoid faraway RF clutters, the distance resolution and the detection coverage of our mmWave radar is set to 4 cm and 3 m, respectively.
2. We conduct a 64-point Fast Fourier transform (FFT) to calculate the frequency components of each segment. Before FFT calculation, we apply Hamming windows to mitigate the spectral leakage.
3. We identify the most informative region (7 data points) of the FFT spectrum by applying a Continuous Wavelet Transform (CWT)-based peak detection algorithm. We observe that these peak regions are representative of different materials. Therefore, instead of feeding the whole FFT spectrum to an ML model for classification, we only extract the region of the peak FFT spectrum, which is easier for the ML model to learn.
4. We extend the 7 data points from the peak spectrum to 13 points by three-point parabolic interpolation. This is because the frequency context from a single channel is coarse-grained, as the 4cm resolution is not precise enough. As a result, we extract a 1D feature of 13 numbers for each Tx-Rx pair.
5. We concatenate the 1D feature from each Tx-Rx pair into a longer 1D feature map [17]. For example, our mmWave radar has 4 receiver antennas and thus the final 1D feature has 52 (4×13) numbers. Since Rx antennas are separated about 2.5 mm apart, which is larger than the mmWave half wavelength (1.9 mm), the channel conditions captured by different Tx-Rx pair varies due to multi-path effect [27]. Therefore, by concatenating features from different Tx-Rx pairs, we obtain a more “panorama” view of the wireless channels and thus better classification accuracy.

3.4 Machine Learning Models

We apply two kinds of machine learning models to classify the materials based on the extracted feature maps. (1) Support Vector Machine (SVM), as it is one of the most well-defined supervised learning models [25]. (2) Convolutional Neural Network (CNN) [22]. We customize a 7-layer CNN as shown in Table 1. For the 1D convolutional layer, we set kernel size to 5 with stride to 1, as a smaller kernel is more perceived to edge information. The first three fully-connected layers have 64 neurons, and the fourth fully-connected layer has 5 outputs (the number of materials in our experiments) [22]. Last, a softmax layer is appended and the material is classified to the output class with the highest probability.

Table 1. Our customized CNN model structure.

Layer	Type	Output shape
0	Input Layer	(52, 1)
1	Conv1D	(48, 1)
2	Conv1D	(44, 1)
3	Conv1D	(40, 1)
4	Fully-Connected Layer	(64)
5	Fully-Connected Layer	(64)
6	Fully-Connected Layer	(64)
7	Fully-Connected Layer	(5)

4 Evaluation

In this section, we first introduce the hardware setup of our system. Then, we explain our collected data set, which is used for the system evaluation. Last, we present our evaluation results.

4.1 Implementation

Figure 4 shows the experiment setup in a corridor. The material plate is mounted on a tripod. The mmWave radar is placed at 40 cm away from the target material plate, with signals transmitted directly to the material plate. In addition, we attach a vibrator motor to the bottom of the mmWave board tripod to mimic the hand-held case. The mmWave radar could be mounted on a mobile robot to search for an optimal distance between the material plate and the mmWave board, which we leave as future work.

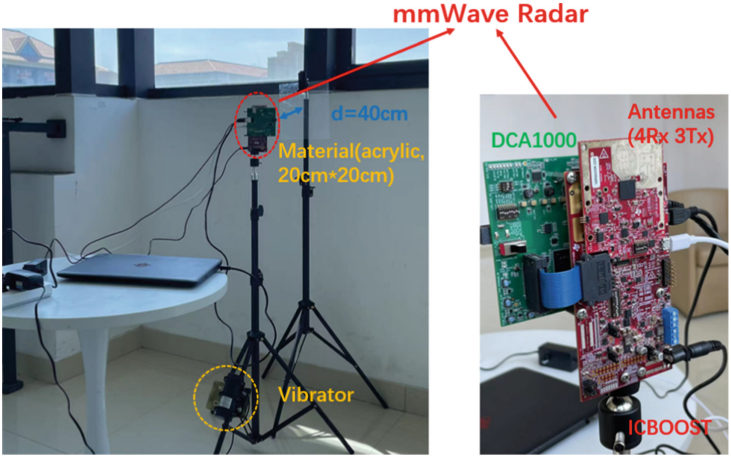


Fig. 4. Experiment setup

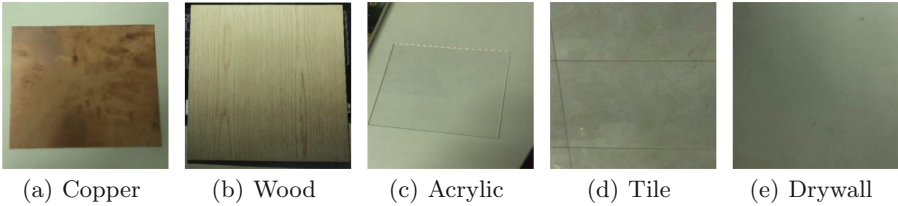


Fig. 5. Materials used for evaluation.

We use a TI IWR1642 Booster Pack that includes an evaluation board (IWR1642BOOST) and a real-time data-capture adapter (DCA1000EVM). The evaluation board has two Tx and four Rx antennas in the 76–81 GHz working frequency range. We use one Tx antenna to transmit the FMCW signal and all four Rx antennas to receive the reflected signal. The antenna chip is directly connected to a laptop (an Intel Core i7-10750H CPU and a 16 GB memory) through two Micro USB cables, and the DCA1000 data capturer is connected to it via an Ethernet RJ45 interface. ICBOOST is supported by a 5V/3A AC power supply adapter, and a 12V/2A adapter powers the vibrator. We use mmWave studio and Matlab for system configuration and data processing.

We select five most common building materials in our experiments. Figure 5 illustrates our chosen material plates, i.e., copper, wood, acrylic, tile, and drywall. Each plate is square in shape, with 20 cm in length/width and 1mm thickness.

4.2 Data Collection and ML Training Configuration

We enable the vibrator to enforce a slight vibration during data collection. In our experiments, we collect raw ADC data stream by the data-capture adapter,

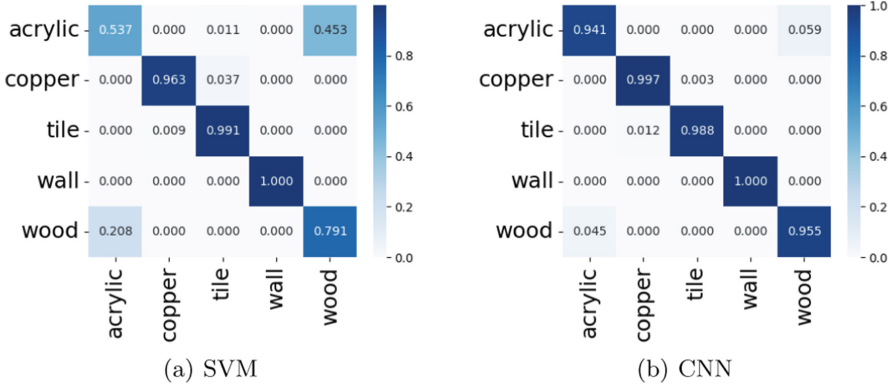


Fig. 6. Confusion matrices of material classification using (a) SVM model and (b) our customized CNN model.

whose sampling rate is set to 3048 KHz. A range resolution up to 4 cm is obtained. In total, we collect 200K data samples from different locations, where each type of material has 40K data samples. Each data sample is an array of 13 floating numbers, and the peak value is located in the center. The total file size of our collected dataset is more than 2 GB.

For the SVM model, we use the default configurations in Matlab. Regarding the CNN model, we adopt the Adam optimizer [12], with a learning rate of 0.001. We apply 10-fold cross-validation and report the average results.

4.3 Evaluation Results

Figure 6 depict the confusion matrices of our mmWave-based material classification system using two different types of ML models. Overall, both models achieve good classification accuracy, as the diagonal cells are much darker than the non-diagonal cells. In particular, our CNN model obtains excellent performance in classifying these materials. In comparison, the SVM model is moderately confused about acrylic and wood. The results indicate that the CNN model structure is powerful for the mmWave-based material classification.

Table 2. SVM (left) and CNN (right) evaluation metrics.

	Accuracy	Precision	Recall	F ₁		Accuracy	Precision	Recall	F ₁
Acrylic	0.86	0.72	0.54	0.62	Acrylic	0.98	0.94	0.95	0.94
Copper		0.99	0.96	0.97	Copper		0.99	0.98	0.98
Tile		0.95	0.99	0.97	Tile		0.98	0.99	0.98
Wall		0.99	0.99	0.99	Wall		1	1	1
Wood		0.64	0.79	0.71	Wood		0.95	0.94	0.94

Table 2 shows the details of the classification performance when the SVM model and the CNN model are applied, respectively. In addition to the average accuracy, we also report the precision, recall, and F_1 score for each type of material. On average, our CNN-based system achieves an inspiring 98% accuracy in classifying these five materials. In addition, our CNN-based system has almost perfect precision, recall, and F_1 , with scores all higher than 0.94.

5 Discussion

Although our system achieves approximately perfect accuracy in classifying materials in our experiments, it has several limitations/opportunities worth further investigation.

Recognizing more Types and Forms of Materials. We select the five most common solid materials in buildings. The chosen materials are diverse, and thus our results are representative. Nonetheless, we plan to evaluate our system with more types of materials such as organic material, and even more forms of materials, including liquid and gas [4, 10, 18].

Support of Dynamic Number of Receiver Antennas. In our current implementation, we fix the number of receiver antennas. As a result, the size of the extracted features and the corresponding ML model are kept the same, which may not be appropriate for other mmWave hardware equipped with a different number of receiver antennas. Therefore, we will design an ML component that supports a dynamic number of antennas. Besides, we will study the classification accuracy versus the number of antennas in our future work.

Developing Finer Feature Engineering. We propose a feature engineering component, which extracts the region around the spectrum peak [9]. In our future work, we want to explore other feature extraction procedures. For example, instead of the 1D spectrum, we can also extract the 2D spectrogram features, which could contain more related information for material recognition.

Support of Less Controlled Experiment Settings. We want to evaluate our system in more dynamic and practical settings. For example, we currently fix the distance between the mmWave board and the material, showing excellent classification accuracy. In our future work, we want to relax this physical constraint so that users can place our mmWave board at various distances from the target material.

6 Conclusion

This paper presents an accurate contact-free material recognition system by leveraging millimeter wave communication and machine learning technology, which is verified efficient in the static indoor material experiment. mmWave has a better sensing capability than other RF technologies because the wavelength of mmWave is much shorter. To extract informative features from mmWave

signals, we propose a unique feature engineering procedure that incorporates frequency domain operations. The extracted features along with our customized CNN model achieves 98% accuracy in classifying five building materials. Our material recognition system is promising considering its high accuracy, low cost, and small size, thanks to the mass-production of mmWave modules. We leave it as future work to design a mobile version of it.

References

1. Adib, F.M., Kabelac, Z., Katabi, D.: Multi-person localization via RF body reflections. In: Proceedings of the 12th USENIX Conference on Networked Systems Design and Implementation (NSDI), pp. 279–292 (2015)
2. Barowski, J., Zimmermanns, M., Rolfes, I.: Millimeter-wave characterization of dielectric materials using calibrated FMCW transceivers. *IEEE Trans. Microw. Theory Tech.* **66**(8), 3683–3689 (2018)
3. Cesetti, M., Nicolosi, P.: Waste processing: new near infrared technologies for material identification and selection. *J. Instrum.* **11**(9), C09002–C09002 (2016)
4. Dhekne, A., Gowda, M.K., Zhao, Y., Hassanieh, H., Choudhury, R.R.: LiquidID: a wireless liquid identifier. In: Proceedings of the 16th Annual International Conference on Mobile Systems, Applications, and Services (MobiSys), pp. 442–454 (2018)
5. Ding, H., et al.: A platform for free-weight exercise monitoring with passive tags. *IEEE Trans. Mob. Comput.* **16**(12), 3279–3293 (2017)
6. Feng, C., et al.: WiMi: target material identification with commodity Wi-Fi devices. In: 2019 IEEE 39th International Conference on Distributed Computing Systems (ICDCS), pp. 700–710 (2019)
7. Harrison, C., Hudson, S.E.: Lightweight material detection for placement-aware mobile computing. In: Proceedings of the 21st Annual ACM Symposium on User Interface Software and Technology (UIST), pp. 279–282 (2008)
8. Heunisch, S., Ohlsson, L., Wernersson, L.E.: Reflection of coherent millimeter-wave wavelets on dispersive materials: a study on porcine skin. *IEEE Trans. Microw. Theory Tech.* **66**(4), 2047–2054 (2018)
9. Holloway, C.L., Perini, P.L., Delyser, R.R., Allen, K.C.: Analysis of composite walls and their effects on short-path propagation modeling. *IEEE Trans. Veh. Technol.* **46**(3), 730–738 (2002)
10. Huang, Y., Chen, K., Wang, L., Dong, Y., Huang, Q., Wu, K.: Lili: liquor quality monitoring based on light signals. In: Proceedings of ACM MobiCom, pp. 256–268 (2021)
11. Iqbal, F., et al.: Alcohol sensing and classification using PCF-based sensor. *Sens. Bio-sens. Res.* **30**, 100384 (2020)
12. Kingma, D.P., Ba, J.: Adam: a method for stochastic optimization. *arXiv Learning* (2014)
13. Koike-Akino, T., Wang, P., Pajovic, M., Sun, H., Orlik, P.V.: Fingerprinting-based indoor localization with commercial MMWave WiFi: a deep learning approach. *IEEE Access* **8**, 84879–84892 (2020)
14. Lin, S.K.: Microwave and millimeter-wave remote sensing for security applications. By Jeffrey A. Nanzer, Artech House, 2012; 372 pages. *Remote. Sens.* **5**, 367–373 (2013)
15. Lu, C.X., et al.: See through smoke: robust indoor mapping with low-cost MMWave radar. In: Proceedings of the 18th International Conference on Mobile Systems, Applications, and Services (MobiSys), pp. 14–27 (2020)

16. Manley, M.: Near-infrared spectroscopy and hyperspectral imaging: non-destructive analysis of biological materials. *Chem. Soc. Rev.* **43**(24), 8200–8214 (2014)
17. das Neves Franco, L.A.P., Sinatora, A.: 3D surface parameters (ISO 25178-2): actual meaning of Spk and its relationship to Vmp. *Precis. Eng.* **40**, 106–111 (2015)
18. Rahman, T., Adams, A.T., Schein, P., Jain, A., Erickson, D., Choudhury, T.: Nutrilizer: a mobile system for characterizing liquid food with photoacoustic effect. In: *Proceedings of ACM SenSys*, pp. 123–136 (2016)
19. Sagala, T.B.V., Suryana, J.: Implementation of mechanical scanning and signal processing for FMCW radar. In: *2016 International Symposium on Electronics and Smart Devices (ISESD)*, pp. 46–50 (2016)
20. Saponaro, P., Sorensen, S., Kolagunda, A., Kambhamettu, C.: Material classification with thermal imagery. In: *2015 IEEE Conference on Computer Vision and Pattern Recognition (CVPR)*, pp. 4649–4656 (2015)
21. Smidt, E., Schwanninger, M., Tintner, J., Böhm, K.: Ageing and deterioration of materials in the environment - application of multivariate data analysis. In: *Multivariate Analysis in Management, Engineering and the Sciences* (2013)
22. Stathakis, D.: How many hidden layers and nodes? *Int. J. Remote Sens.* **30**, 2133–2147 (2009)
23. Vakili, I., Ohlsson, L., Wernersson, L.E., Gustafsson, M.G.: Time-domain system for millimeter-wave material characterization. *IEEE Trans. Microw. Theory Tech.* **63**(9), 2915–2922 (2015)
24. Wang, J., Xiong, J., Chen, X., Jiang, H., Balan, R.K., Fang, D.: TagScan: simultaneous target imaging and material identification with commodity RFID devices. In: *Proceedings of the 23rd Annual International Conference on Mobile Computing and Networking (MobiCom)*, pp. 288–300 (2017)
25. Wu, T., Lin, C.J., Weng, R.C.H.: Probability estimates for multi-class classification by pairwise coupling. *J. Mach. Learn. Res.* **5**, 975–1005 (2003)
26. Yang, Z., et al.: On the feasibility of estimating soluble sugar content using millimeter-wave. In: *Proceedings of ACM/IEEE IoTDI*, pp. 13–24 (2019)
27. Yanik, M.E., Torlak, M.: Near-field MIMO-SAR millimeter-wave imaging with sparsely sampled aperture data. *IEEE Access* **7**, 31801–31819 (2019)
28. Yeo, H.S., Flamich, G., Schrempf, P., Harris-Birtill, D., Quigley, A.J.: Radarcat: radar categorization for input interaction. In: *Proceedings of the 29th Annual Symposium on User Interface Software and Technology (UIST)*, pp. 833–841 (2016)
29. Zhang, R., Cao, S.: Extending reliability of mmWave radar tracking and detection via fusion with camera. *IEEE Access* **7**, 137065–137079 (2019)
30. Zhao, M., et al.: RF-based 3D skeletons. In: *Proceedings of the 2018 Conference of the ACM Special Interest Group on Data Communication (SIGCOMM)*, pp. 267–281 (2018)
31. Zhu, Y., Zhu, Y., Zhao, B.Y., Zheng, H.: Reusing 60ghz radios for mobile radar imaging. In: *Proceedings of the 21st Annual International Conference on Mobile Computing and Networking (MobiCom)*, pp. 103–116 (2015)